A NEW METHOD FOR LAPLACE'S EQUATION IN TWO-DIMENSIONAL REGIONS WITH CIRCULAR HOLES

Wen-Cheng Shen[1], Kue-Hong Chen[2], Jeng-Tzong Chen[1]
[1]*Department of Harbor and River Engineering, National Taiwan Ocean University*
[2]*Department of Information Management, Toko University*
wave@msvlab.hre.ntou.edu.tw

ABSTRACT

This paper describes a numerical procedure for solving the Laplace problems of circular domain containing multiple circular holes by using the null-field integral equation, Fourier series and degenerate kernels. The unknown boundary potential and flux are approximated by using the truncated Fourier series. Degenerate kernels for the fundamental solutions are utilized in the boundary integral equation. A linear algebraic system is obtained without boundary discretization. Degenerate scale in the multiply-connected domain is also examined. Several examples are illustrated and the results are compared well with the exact solution and those of Caulk's data.

Keywords: multiple circular holes, Laplace problem, null-field integral equation, degenerate kernel, Fourier series

INTRODUCTION

A number of engineering problems require the solutions of Laplace's equation in regions with circular holes, e.g. steady state heat conduction of tube [1], flow of incompressible flow around cylinders, electrostatic fields of wires and torsion bar with holes. Although analytical methods involve special mapping technique or restricted solution representations, only limited cases were solved. Numerical methods are always resorted to deal with the problems. Finite element method (FEM) has been commonly employed to solve such problems, but a large number of elements are required to model this region. To reduce the effort of mesh generation, boundary element method (BEM) is also an efficient alternative which has been extensively used [2]. Caulk and his coworkers [1, 3, 4] have adopted the Fourier series in his special boundary integral method. Bird and Steele also utilized Fourier series for harmonic and biharmonic problems with circular holes [5-6]. Wang *et al.* also employed complex Fourier series and complex variable boundary integral equation method (BIEM) to handle elasticity problems with circular boundaries [7]. However, they did not employ the null-field integral equation and degenerate kernels to fully capture the circular boundary. Shen *et al.* have proposed a new method to deal with the half-plane [8] or infinite-plane problems [9] with circular holes. Null-field integral equation in conjunction with the degenerate kernels and Fourier series are fully incorporated to capture the circular geometry.

In this paper, BIEM is utilized to solve problems with multiple circular boundaries. To utilize the geometry of circular boundary, Fourier series for boundary densities and degenerate kernels for fundamental solutions are incorporated into the null-field integral equation. The unknown boundary potential and flux are approximated by using the truncated Fourier series. By matching the boundary condition, the unknown Fourier coefficients can be determined by substituting the degenerate

kernels into the null-field integral equation. Numerical results are given to illustrate the validity of the present approach. The accuracy and efficiency for the present method are also examined.

PROBLEM STATEMENT AND INTEGRAL FORMULATION

Consider the Laplace problem with a circular domain containing N randomly distributed circular holes centered at position vector $\underset{\sim}{c}_j$ (j =1, 2, ..., N) as shown in Fig. 1. Let a_j and B_j denote the radius and boundary of the jth circular hole.

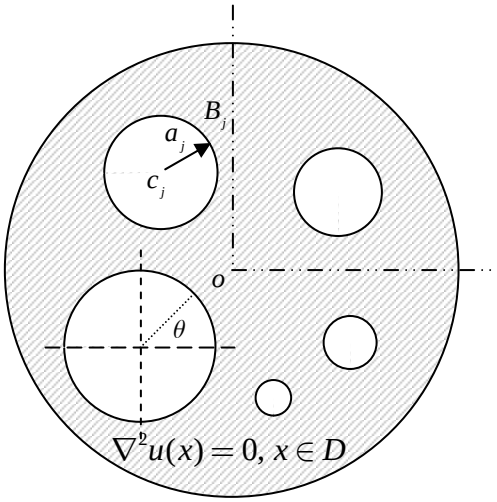

FIGURE 1 Problem statement

By employing the Fourier series expansions to approximate the potential u and its normal flux t on the boundary, we have

$$u(\underset{\sim}{s}) = a_{0j} + \sum_{n=1}^{\infty}(a_{nj}\cos n\theta_j + b_{nj}\sin n\theta_j),\ \underset{\sim}{s} \in B_j \tag{1}$$

$$t(\underset{\sim}{s}) = p_{0j} + \sum_{n=1}^{\infty}(p_{nj}\cos n\theta_j + q_{nj}\sin n\theta_j),\ \underset{\sim}{s} \in B_j \tag{2}$$

where a_{0j}, a_{nj}, b_{nj}, p_{0j}, p_{nj} and q_{nj} are the coefficients, θ_j is the polar angle centered at c_j. Based on the boundary integral formulation of the domain point for the potential problem [10], we have

$$2\pi u(\underset{\sim}{x}) = \int_B T(\underset{\sim}{s},\underset{\sim}{x})u(\underset{\sim}{s})dB(\underset{\sim}{s}) - \int_B U(\underset{\sim}{s},\underset{\sim}{x})t(\underset{\sim}{s})dB(\underset{\sim}{s}),\ \underset{\sim}{x} \in D \tag{3}$$

where $t(\underset{\sim}{s}) = \partial u(\underset{\sim}{s})/\partial n_{\underset{\sim}{s}}$, $\underset{\sim}{s}$ and $\underset{\sim}{x}$ are the source and field points, respectively, D is the domain of interest, B is the boundary and $U(\underset{\sim}{s},\underset{\sim}{x}) = \ln r$ ($r = \left|\underset{\sim}{x} - \underset{\sim}{s}\right|$) , is the fundamental solution which satisfies

$$\nabla^2 U(\underset{\sim}{x},\underset{\sim}{s}) = 2\pi\delta(\underset{\sim}{x} - \underset{\sim}{s}) \tag{4}$$

in which, $\delta(\underset{\sim}{x} - \underset{\sim}{s})$ denotes the Dirac-delta function. $T(\underset{\sim}{s},\underset{\sim}{x})$ is defined by

$$T(\underset{\sim}{s},\underset{\sim}{x}) = \frac{\partial U(\underset{\sim}{s},\underset{\sim}{x})}{\partial n_{\underset{\sim}{s}}} \tag{5}$$

where $n_{\underset{\sim}{s}}$ denotes the outward normal vector at the source point s. By collocating $\underset{\sim}{x}$ outside the domain ($\underset{\sim}{x} \in D^e$), we obtain the null-field integral equation as shown below

$$0 = \int_B T(\underset{\sim}{s},\underset{\sim}{x})u(\underset{\sim}{s})dB(\underset{\sim}{s}) - \int_B U(\underset{\sim}{s},\underset{\sim}{x})t(\underset{\sim}{s})dB(\underset{\sim}{s}),\ \underset{\sim}{x} \in D^e \tag{6}$$

Based on the separable property, the U kernel function can be expanded into degenerate form as shown below

$$U(\underset{\sim}{s},\underset{\sim}{x}) = \begin{cases} U^i = \ln\left|\underset{\sim}{s} - \underset{\sim}{c}_j\right| - \sum_{m=1}^{\infty}\frac{1}{m}\left(\frac{\left|\underset{\sim}{x} - \underset{\sim}{c}_j\right|}{\left|\underset{\sim}{s} - \underset{\sim}{c}_j\right|}\right)^m \cos m\alpha, \\ \qquad \left|\underset{\sim}{s} - \underset{\sim}{c}_j\right| > \left|\underset{\sim}{x} - \underset{\sim}{c}_j\right| \\ U^e = \ln\left|\underset{\sim}{x} - \underset{\sim}{c}_j\right| - \sum_{m=1}^{\infty}\frac{1}{m}\left(\frac{\left|\underset{\sim}{s} - \underset{\sim}{c}_j\right|}{\left|\underset{\sim}{x} - \underset{\sim}{c}_j\right|}\right)^m \cos m\alpha, \\ \qquad \left|\underset{\sim}{x} - \underset{\sim}{c}_j\right| > \left|\underset{\sim}{s} - \underset{\sim}{c}_j\right| \end{cases} \tag{7}$$

where α is the angle between $\underset{\sim}{s} - \underset{\sim}{c}_j$ and $\underset{\sim}{x} - \underset{\sim}{c}_j$, the superscripts i and e denote the interior and exterior cases, respectively. After taking the normal derivative, the $T(\underset{\sim}{s},\underset{\sim}{x})$ kernel can be derived as

$$T(\underset{\sim}{s},\underset{\sim}{x}) = \begin{cases} T^i = \dfrac{1}{\left|\underset{\sim}{s}-\underset{\sim}{c}_j\right|} + \sum_{m=1}^{\infty}\left(\dfrac{\left|\underset{\sim}{x}-\underset{\sim}{c}_j\right|^m}{\left|\underset{\sim}{s}-\underset{\sim}{c}_j\right|^{m+1}}\right)\cos m\alpha, \\ \qquad\qquad \left|\underset{\sim}{s}-\underset{\sim}{c}_j\right| > \left|\underset{\sim}{x}-\underset{\sim}{c}_j\right| \\ T^e = -\sum_{m=1}^{\infty}\left(\dfrac{\left|\underset{\sim}{s}-\underset{\sim}{c}_j\right|^{m-1}}{\left|\underset{\sim}{x}-\underset{\sim}{c}_j\right|^m}\right)\cos m\alpha, \\ \qquad\qquad \left|\underset{\sim}{x}-\underset{\sim}{c}_j\right| > \left|\underset{\sim}{s}-\underset{\sim}{c}_j\right| \end{cases} \quad (8)$$

In the real computation, only finite M terms are used in the summation of Eqs. (1) and (2).

LINEAR ALGEBRAIC SYSTEM

By collocating the null-field point $\left|\underset{\sim}{x}_k-\underset{\sim}{c}_j\right| = a_k^-$ on the *kth* circular boundary for Eq. (6), we have

$$0 = \sum_{j=1}^{N_c}\int_{B_j} T(\underset{\sim}{s},\underset{\sim}{x}_k)u(\underset{\sim}{s})dB(\underset{\sim}{s}) - \sum_{j=1}^{N_c}\int_{B_j} U(\underset{\sim}{s},\underset{\sim}{x}_k)t(\underset{\sim}{s})dB(\underset{\sim}{s}),\ \underset{\sim}{x}\in D^e \quad (9)$$

where N_c is the number of circles. It is noted that the path is counterclockwise for the outer circle. Otherwise, it is clockwise. For the B_j integral of the circular boundary, the kernels of $U(\underset{\sim}{s},\underset{\sim}{x})$ and $T(\underset{\sim}{s},\underset{\sim}{x})$ are respectively expressed in terms of degenerate kernels of Eqs. (7) and (8), and $u(\underset{\sim}{s})$ and $t(\underset{\sim}{s})$ are substituted by using the Fourier series of Eqs. (1) and (2), respectively. In the B_j integration, we set the origin of the observer system to collocate at the center c_j to fully utilize the degenerate kernel and Fourier series. By collocating the null-field point near B_k, Fig. 2 (a) shows the collocation point and boundary contour. A linear algebraic system is obtained

$$[U]\{x\} = [T]\{y\} \quad (10)$$

where $[U]$ and $[T]$ are the influence matrices, $\{x\}$ and $\{y\}$ denote the vectors of Fourier coefficients, respectively. By rearranging the known and unknown sets, the unknown Fourier coefficients are determined. After obtaining the unknown Fourier coefficients, the origin of observer system is set to c_j in the B_j integration as shown in Fig. 2 (b) to obtain the interior potential by employing Eq. (3). The boundary integrals on the circle are listed in the Appendix. The flow chart of the present method is shown in Fig. 3.

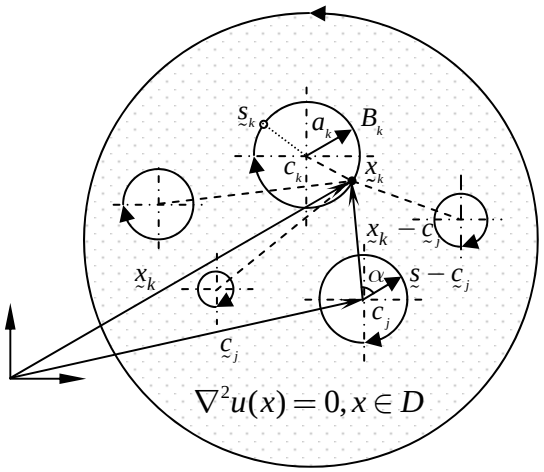

FIGURE 2 (a) Null-field integral equation

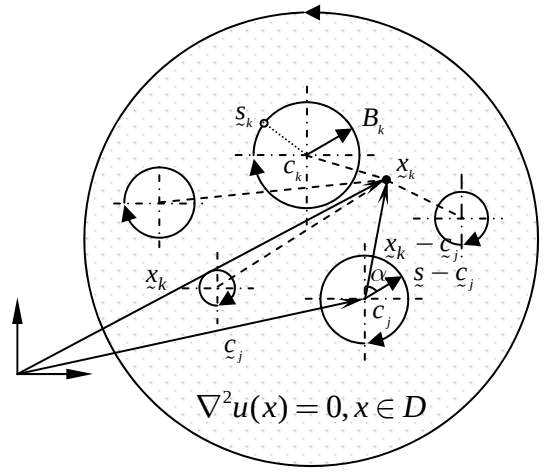

FIGURE 2 (b) Boundary integral equation for the domain point

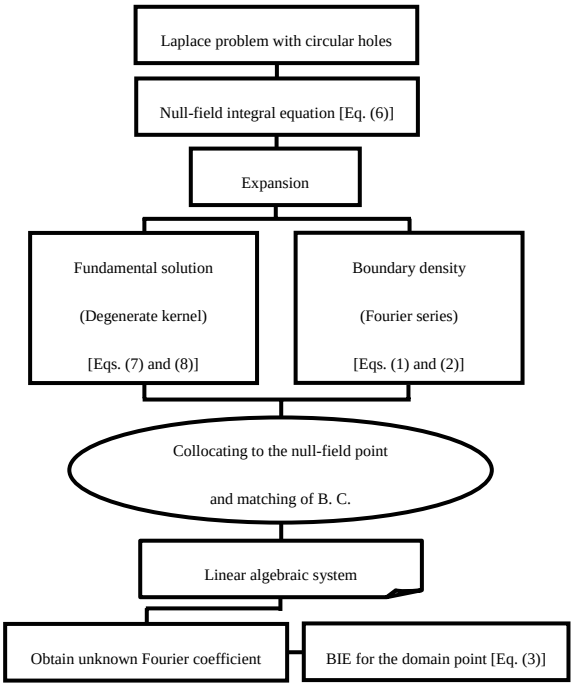

FIGURE 3 The flow chart of the present method

DISCUSSIONS ON DEGENERATE SCALE

When the outer boundary has a radius of one ($a=1$), the null-field integral equation results in

$$\begin{bmatrix} \cdots & 2\pi a\ln a & \cdots \\ \vdots & \vdots & \vdots \\ \cdots & 2\pi a\ln a & \cdots \end{bmatrix} \begin{Bmatrix} \vdots \\ p_{oj} \\ p_{mj} \\ q_{mj} \\ \vdots \end{Bmatrix} = [T] \begin{Bmatrix} \vdots \\ a_{oj} \\ a_{mj} \\ b_{mj} \\ \vdots \end{Bmatrix} \qquad (11)$$

no matter what the null-field point is collocated due to the property of degenerate kernel in Eq. (7). As the radius a is one, the influence matrix is singular for the Dirichlet problem. This finding extends the proof of annular case where the outer radius of one is a degenerate scale [11-14]. No matter how many inner holes are located inside the outer boundary, the Dirichlet problem with radius one of the outer boundary is not solvable due to rank deficiency in Eq. (11). To avoid the nonuniqueness for the BIE formulation, all the outer radii of the following examples are not equal to one to avoid the degenerate scale.

NUMERICAL RESULTS

In order to demonstrate the validity of the present method. Several examples are given.

Example 1. An eccentric case with radii a_1 and a_2 ($a_1=1$, $a_2=2.5$) is shown in Fig. 4 (a). The boundary condition on the hole is $u=0$ and the potential on the outer circle is one. The numerical result is shown in Fig. 4 (b). Good agreement is made after comparing well with the exact solution [15],

$$u(\rho,\phi)=\frac{1}{2\ln 2}\ln\left[\frac{16\rho^2+1+8\rho\cos\phi}{\rho^2+16+8\rho\cos\phi}\right] \qquad (12)$$

as shown in Fig. 4 (c).

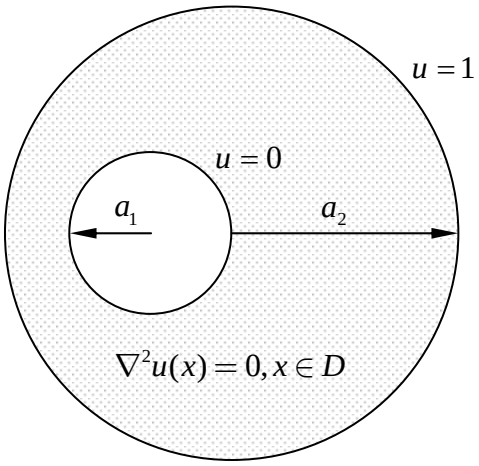

FIGURE 4 (a) A circular domain with an eccentric circle

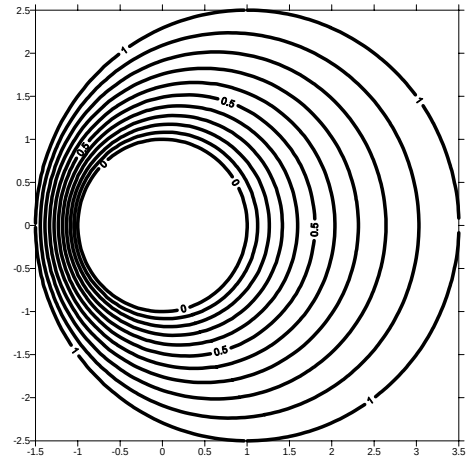

FIGURE 4 (b) Contour of potential (M=10)

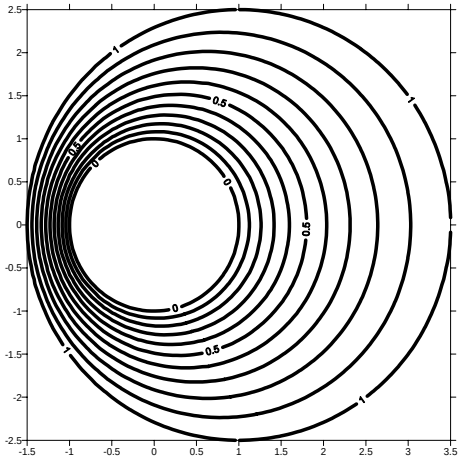

FIGURE 4 (c) Exact solution [15]

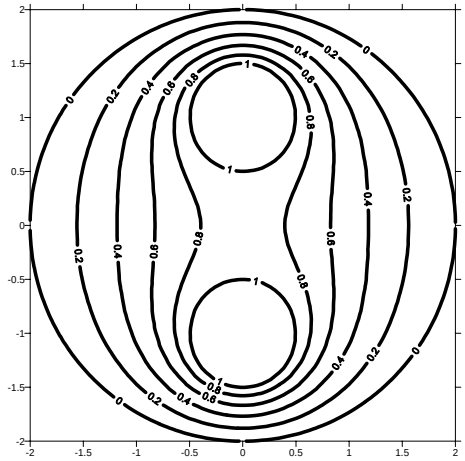

FIGURE 5 (b) Contour of potential (M=10)

Example 2. A circular region of radius R with two circular holes which are placed on a concentric circle of radius b ($b=1$). Both holes have the same radius a as shown in Fig. 5 (a). The radii of the circular holes and the external boundary are $a=0.5$ and $R=2$. The results are shown in Fig. 5 (b). After comparing with the quarter part of Caulk's result in Fig. 5 (c) [1], good agreement is made.

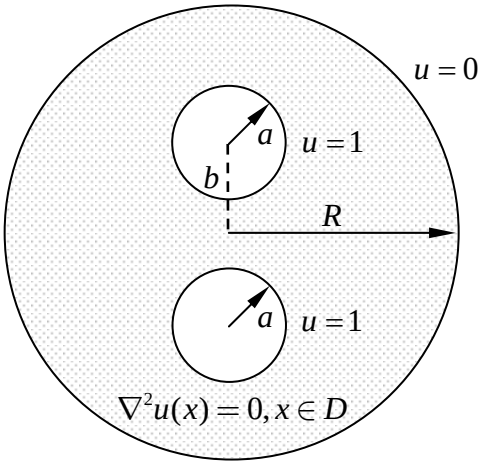

FIGURE 5 (a) Two circular holes in a circular domain

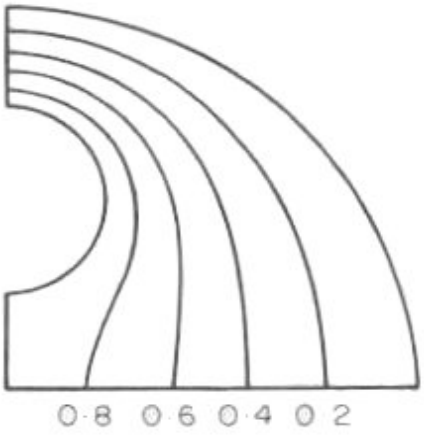

FIGURE 5 (c) Quarter part of the potential by Caulk [1]

Example 3. Consider the same region as the above example, but now add a hole of radius c at the center. The boundary conditions are different from each other as shown in Fig. 6 (a). The radii of the holes are $a=c=0.4$ and the distance $b=1.2$ from the center of the external boundary. Fig. 6 (b) shows the numerical results obtained using the present method. The quarter part of the potential by Caulk [1] is shown in Fig. 6 (c) for comparison, good agreement is made.

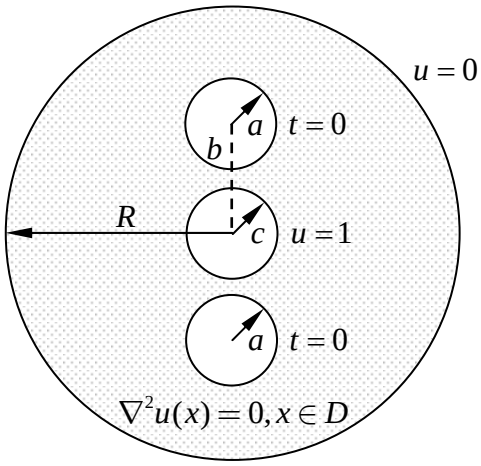

FIGURE 6 (a) Three circular holes in a circular domain

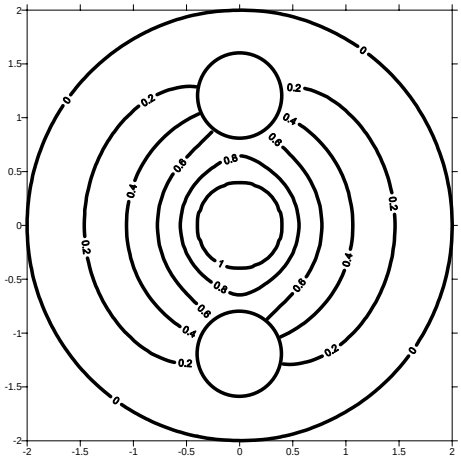

FIGURE 6 (b) Contour of potential (M=10)

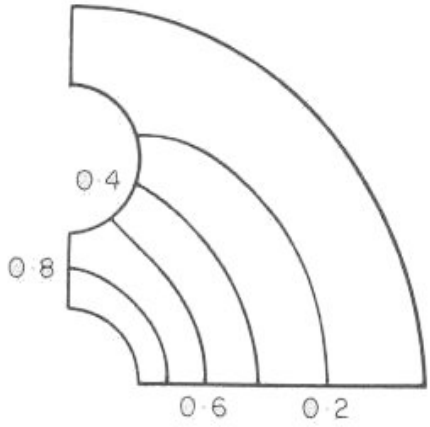

FIGURE 6 (c) Quarter part of the potential by Caulk [1]

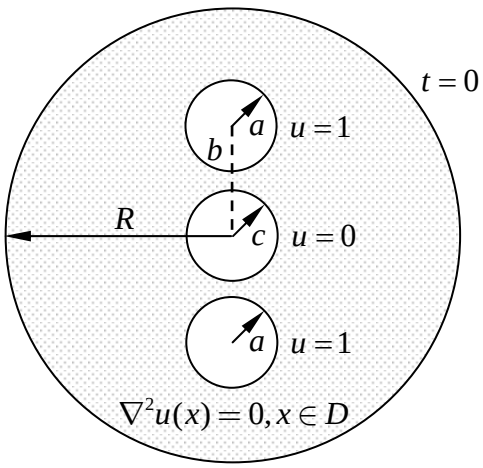

FIGURE 7 (a) Three circular holes in a circular domain

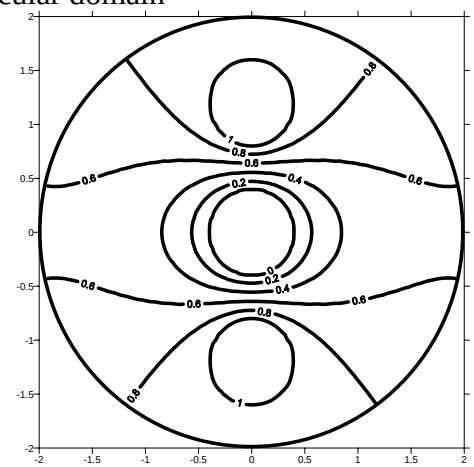

FIGURE 7 (b) Contour of potential (M=10)

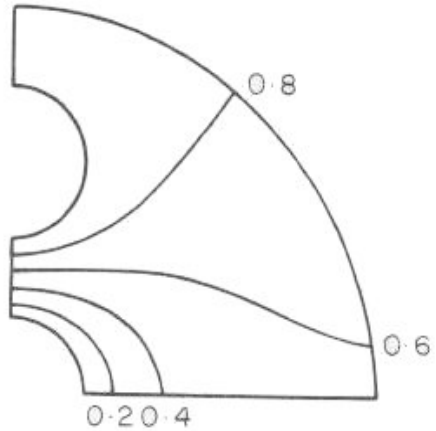

FIGURE 7 (c) Quarter part of the potential by Caulk [1]

Example 4. By changing the boundary conditions of example 3, we have example 4 as shown in Fig. 7 (a). The results in Fig. 7 (b) are compared well with the quarter part of Caulk's data in Fig. 7 (c).

In all the examples, only ten terms of Fourier series (M=10) were needed to converge well with the exact solution [15] for example 1 and Caulk's data for examples 2, 3 and 4 [1]. The present method is more accurate for the Laplace problems with multiple circular holes than others (FEM or

BEM) under the same number of degrees of freedoms.

CONCLUSIONS

For the Laplace problems with circular boundaries, we have proposed a special BIEM by using degenerate kernels, null-field integral equation and Fourier series in an adaptive observer system. The method shows great generality and versatility for the problems with multiple circular holes of arbitrary radii and positions. The degenerate scale is also discussed for the multiply-connected case. Numerical results agree very well with the available exact solution and Caulk's data.

REFERENCES

1. Caulk, D. A., "Analysis of Steady Heat Conduction in Regions with Circular Holes by a Special Boundary-Integral Method", *IMA Journal of Applied Mathematics* Vol. 30, pp. 231-246, (1983).
2. 陳正宗與洪宏基, "邊界元素法", 第二版, *新世界出版社*, 台北, (1992).
3. Barone, M. R. and Caulk, D. A., Special Boundary Integral Equations for Approximate Solution of Laplace's Equation in Two-dimensional Regions with Circular Holes, *Quarterly Journal of Mechanics and Applied Mathematics*, Vol. 34, pp. 265-286, (1981).
4. Caulk, D. A., "Special Boundary Integral Equations for Potential Problems in Regions with Circular Holes", *Journal of Applied Mechanics*, Vol. 51, pp. 713-716, (1984).
5. Bird, M. D. and Steele, C. R., "A Solution Procedure for Laplace's Equation on Multiply-Connected Circular Domains", *Journal of Applied Mechanics*, Vol. 59, pp. 398-404, (1992).
6. Bird, M. D. and Steele, C. R., "Separated Solution Procedure for Bending of Circular Plates with Circular Holes", *Applied Mechanics Reviews*, Vol. 44, pp. 27-35, (1991).
7. Wang, J., Mogilevskaya, S. G. and Crouch, S. L., "A Numerical Procedure for Multiple Circular Holes and Elastic Inclusions in a Finite Domain with a Circular Boundary", *Computational Mechanics*, Vol. 32, pp. 250-258, (2002).
8. Shen, W. C., Lee, C. F. and Chen, J. T., "A Study on Half-Plane Laplace Problems with a Circular Hole", *The 7th National Conference on Structure Engineering*, Chung-Li, (2004).
9. Shen, W. C., Lee, C. F. and Chen, J. T., "A study on Laplace Problems of Infinite Plane with Multiple Circular Holes", *The International Conference on Computational Methods*, Singapore, (2004)
10. Chen, J. T. and Hong, H.-K., "Review of Dual Boundary Element Methods with Eemphasis on Hypersingular Integrals and Divergent Series", *Applied Mechanics Reviews, ASME*, Vol. 52, pp. 17-33, (1999).
11. Chen, J. T., Kuo, S. R. and Lin, J. H., "Analytical study and numerical experiments for degenerate scale problems in the boundary element method for two-dimensional elasticity", *International Journal for Numerical Methods in Engineering*, Vol. 54, pp. 1669-1681, (2002).
12. Chen, J. T., Lee, C. F., Chen, I. L. and Lin, J. H., "An alternative method for degenerate scale problem in boundary element methods for the two-dimensional Laplace equation", *Engineering Analysis with Boundary Elements*, Vol. 26, pp. 559-569, (2002).
13. Chen, J. T., Lin, J. H., Kuo, S. R. and Chiu, Y. P., "Analytical study and numerical experiments for degenerate scale problems in boundary element method using degenerate kernels and circulants", *Engineering Analysis with Boundary Elements*, Vol. 25, pp. 819-828, (2001).

14. Chen, J. T., Lin, S. R. and Chen, K. H., "Degenerate scale problem when solving Laplace's equation by BEM and its treatment", *International Journal for Numerical Methods in Engineering*, Accepted, (2004).
15. Carrier, G. F. and Pearson, C. E., "Partial Differential Equations", *Academic Press*, New York, (1976).

APPENDIX

(1) For the null-field integral equation of Eq. (6) in Fig. 2 (a), we have ($\left|\underset{\sim}{s}-\underset{\sim}{c}_j\right|>\left|\underset{\sim}{x}-\underset{\sim}{c}_j\right|$).

$$\int_{B_j} U(\underset{\sim}{s},\underset{\sim}{x})t(\underset{\sim}{s})dB(\underset{\sim}{s})$$

$$=\int_0^{2\pi}[\ln\left|\underset{\sim}{s}-\underset{\sim}{c}_j\right|-\sum_{m=1}^{\infty}\frac{1}{m}(\frac{\left|\underset{\sim}{x}-\underset{\sim}{c}_j\right|}{\left|\underset{\sim}{s}-\underset{\sim}{c}_j\right|})^m\cos m\alpha]$$

$$[p_{oj}+\sum_{n=1`}^{M}(p_{nj}\cos n\theta+q_{nj}\sin n\theta)]a_j d\theta$$

$$=2\pi a_j\ln\left|\underset{\sim}{s}-\underset{\sim}{c}_j\right|p_{oj}$$

$$-\sum_{m=1}^{M}\{\frac{\pi a_j}{m}[p_{mj}(\frac{\left|\underset{\sim}{x}-\underset{\sim}{c}_j\right|}{\left|\underset{\sim}{s}-\underset{\sim}{c}_j\right|})^m\cos m\phi$$

$$+q_{mj}(\frac{\left|\underset{\sim}{x}-\underset{\sim}{c}_j\right|}{\left|\underset{\sim}{s}-\underset{\sim}{c}_j\right|})^m\sin m\phi]\}$$

$$\int_{B_j} T(\underset{\sim}{s},\underset{\sim}{x})u(\underset{\sim}{s})dB(\underset{\sim}{s})$$

$$=\int_0^{2\pi}[\frac{1}{\left|\underset{\sim}{s}-\underset{\sim}{c}_j\right|}+\sum_{m=1}^{\infty}(\frac{\left|\underset{\sim}{x}-\underset{\sim}{c}_j\right|^m}{\left|\underset{\sim}{s}-\underset{\sim}{c}_j\right|^{m+1}})\cos m\alpha]$$

$$[a_{oj}+\sum_{n=1`}^{M}(a_{nj}\cos n\theta+b_{nj}\sin n\theta)]a_j d\theta$$

$$=\frac{2\pi a_j}{\left|\underset{\sim}{s}-\underset{\sim}{c}_j\right|}+\sum_{m=1}^{M}\{\pi a_j[p_{mj}(\frac{\left|\underset{\sim}{x}-\underset{\sim}{c}_j\right|^m}{\left|\underset{\sim}{s}-\underset{\sim}{c}_j\right|^{m+1}})\cos m\phi$$

$$+q_{mj}(\frac{\left|\underset{\sim}{x}-\underset{\sim}{c}_j\right|^m}{\left|\underset{\sim}{s}-\underset{\sim}{c}_j\right|^{m+1}})\sin m\phi]\}$$

(2) For the interior point of Eq. (3) in Fig. 2 (b), we have ($\left|\underset{\sim}{x}-\underset{\sim}{c}_j\right|>\left|\underset{\sim}{s}-\underset{\sim}{c}_j\right|$).

$$\int_{B_j} U(\underset{\sim}{s},\underset{\sim}{x})t(\underset{\sim}{s})dB(\underset{\sim}{s})$$

$$=\int_0^{2\pi}[\ln\left|\underset{\sim}{x}-\underset{\sim}{c}_j\right|-\sum_{m=1}^{\infty}\frac{1}{m}(\frac{\left|\underset{\sim}{s}-\underset{\sim}{c}_j\right|}{\left|\underset{\sim}{x}-\underset{\sim}{c}_j\right|})^m\cos m\alpha]$$

$$[p_{oj}+\sum_{n=1`}^{M}(p_{nj}\cos n\theta+q_{nj}\sin n\theta)]a_j d\theta$$

$$=2\pi a_j\ln\left|\underset{\sim}{x}-\underset{\sim}{c}_j\right|p_{oj}$$

$$-\sum_{m=1}^{M}\{\frac{\pi a_j}{m}[p_{mj}(\frac{\left|\underset{\sim}{s}-\underset{\sim}{c}_j\right|}{\left|\underset{\sim}{x}-\underset{\sim}{c}_j\right|})^m\cos m\phi$$

$$+q_{mj}(\frac{\left|\underset{\sim}{s}-\underset{\sim}{c}_j\right|}{\left|\underset{\sim}{x}-\underset{\sim}{c}_j\right|})^m\sin m\phi]\}$$

$$\int_{B_j} T(\underset{\sim}{s},\underset{\sim}{x})u(\underset{\sim}{s})dB(\underset{\sim}{s})$$

$$=\int_0^{2\pi}[-\sum_{m=1}^{\infty}(\frac{\left|\underset{\sim}{s}-\underset{\sim}{c}_j\right|^{m-1}}{\left|\underset{\sim}{x}-\underset{\sim}{c}_j\right|^m})\cos m\alpha]$$

$$[a_{oj}+\sum_{n=1`}^{M}(a_{nj}\cos n\theta+b_{nj}\sin n\theta)]a_j d\theta$$

$$=-\sum_{m=1}^{M}\{\pi a_j[p_{mj}(\frac{\left|\underset{\sim}{s}-\underset{\sim}{c}_j\right|^{m-1}}{\left|\underset{\sim}{x}-\underset{\sim}{c}_j\right|^m})\cos m\phi$$

$$+q_{mj}(\frac{\left|\underset{\sim}{s}-\underset{\sim}{c}_j\right|^{m-1}}{\left|\underset{\sim}{x}-\underset{\sim}{c}_j\right|^m})\sin m\phi]\}$$

where $\left|\underset{\sim}{s}-\underset{\sim}{c}_j\right|=R$, $\left|\underset{\sim}{x}-\underset{\sim}{c}_j\right|=\rho$, θ and ϕ are shown in Fig. 8.

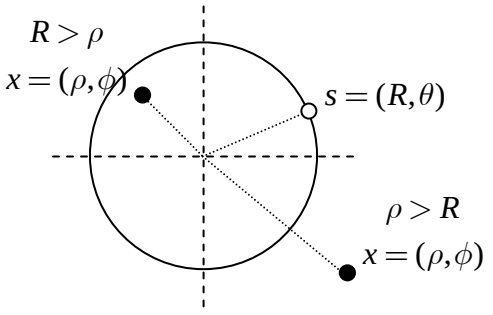

FIGURE 8 Sketch of the source and field points

二維區域含圓洞之
拉普拉斯問題的新解法

沈文成　陳正宗
國立台灣海洋大學河海工程系

摘要

本文以勢能理論為基礎，提出以退化核與傅立葉級數展開搭配零場積分方程求解含多孔洞拉普拉斯問題。此方法可視為半解析法。邊界未知勢能與流通量使用有限項傅立葉級數來近似求得。利用退化核與傅立葉展開可導得一線性代數方法而無須對邊界離散，並對退化尺度進行探討。最後以幾個不同邊界條件的拉普拉斯問題進行測試。所得結果無論與解析解或是與 Caulk 的數值結果比較，均可驗證本方法的正確性。

關鍵字：多孔洞，拉普拉斯問題，零場積分方程式，退化核，傅立葉級數